SUPPLEMENTARY NOTES

Patients

Patients BAB3401 and BAB3402 (family HOU1338) first presented to Cerrahpasa Medical School, Department of Medical Genetics when they were 5 years and 2 years, 9 months old, respectively. Chief complaints for BAB3401 were seizures, inability to walk, lack of speech, and significant sleep disturbance. He was born at term by vaginal delivery without any complication after a pregnancy without prenatal medical care. Anthropometric measurements at birth were as follows; Weight (W): 3400 gr, Length (L): 53cm, Occipitofrontal circumference (OFC): 34 cm (Figure S1A). Initial neurological symptoms were seizures that started in early infancy, and then significant delay in development was reported by the parents. Anthropometric measurements at age 5 year were: W: NA, L: 92cm (<3%), OFC: 45cm (<3%) (Figure S1A). Physical examination showed severe developmental delay/intellectual disability (DD/ID) with neither head control nor unsupported sitting, spasticity in all extremities, poor eye contact, strabismus, and bilateral cryptorchidism (Figure 1). Frequent tonic-clonic seizures were noted. The clinical course of BAB3402 was similar to that for his brother (BAB3401). The patient was born full-term after an apparently uneventful pregnancy. Anthropometric measurements at birth were within normal limits; W: 3150gr (10-25%), L: 51cm (50%), OFC: 34 cm (25-50%) (Figure S1A). Generalized tonic-clonic seizures started shortly after birth. Anthropometric measurements at age 2 years, 9 months were: W: NA, L: 85 cm (<3%), OFC: 44cm (<3%) (Figure S1A). Physical examination revealed no head control and no eye contact. He also exhibited bilateral cryptorchidism. Metabolic tests (blood amino acids and urine organic acids), chromosome analysis, and sub-telomeric MLPA analysis did not reveal any abnormalities in both siblings.

Brain MRI studies of both siblings revealed evidence of microcephaly, brain dysgenesis with generalized volume loss prominently affecting the frontotemporal region, severely delayed myelination, hypoplasia of the corpus callosum (prominent at splenium), and vertical clivus (Figure 1). The most recent physical examination at ages 8 and 6 years revealed significant developmental delay, microcephaly, esotropia, nystagmus and truncal hypotonia, spasticity with brisk DTRs in the upper extremities, and lower limb hypotonia with intact DTRs. Electrophysiological studies revealed axonal sensorimotor neuropathies (Figure 2, Table S1). The patients' seizures were persistent and unresponsive to anticonvulsive drugs. In addition to neurologic findings, the patients showed facial dysmorphism characterized by high arched eyebrows, prominent eyes with long palpebral fissures and eyelashes, prominent broad nose root, short nose, hypoplastic alae nasi, and thin upper lips with a narrow-high arched palate (Figure 1).

Patients BAB3421 and BAB3422 (family HOU1333) were initially referred to the Metabolic Disorders clinic by their primary care physician with a preliminary diagnosis of neurometabolic disorder because of seizures, DD/ID and brain abnormalities at ages 5 years, 6 months and 3 years, 9 months, respectively. Initial metabolic workup including tandem mass spectrometry, urine organic acids, and blood amino acid levels were within normal ranges. The patients were subsequently referred to the Medical Genetic department due to abnormal brain MRIs, neuro-developmental delay and dysmorphic features. Both pregnancies and deliveries were not under the supervision of a physician, but according to parental reports, both siblings were born at home uneventfully after full term gestations. Both siblings had generalized tonic-clonic seizures within the first few months of life that were refractory to medical treatment. Anthropometric measurements at ages 5 years, 6 months and 3 years, 9 months years revealed that all

measurements were less than the 3rd percentile (BAB3421 W: 12.8 kg, L: 87 cm, OFC: 44 cm / BAB3422 W: 11.7 kg, L: 83 cm, OFC: 43.7 cm) (Figure S1A). Clinical evaluation revealed severe DD/ID, microcephaly (Figure S1A), nystagmus, truncal hypotonia and spasticity in all four extremities. Facial dysmorphic features including high arched eyebrows, long palpebral fissures and eyelashes with prominent eyes, prominent-broad nasal root, short nose with upturned nostrils and hypoplasic alae nasi were noted (Figure 1). Brain MRI studies at ages 3 years, 9 months and 2 years, 1 month showed cortical atrophy that is prominent at the fronto-temporal region, hypoplastic corpus callosum, and accompanying vertical clivus (Figure 1). Electrophysiological studies demonstrated sensorimotor neuropathy (Figure 2 and Table S1).

Two members of family HOU1926 (BAB4770 and BAB4771) were referred to Cerrahpasa Medical School, Department of Medical Genetics at ages 7 years, 3 months and 4 years, 11 months, respectively. The presenting complaints of both siblings were inability to walk, lack of speech, and seizures. Pre- and natal records were unavailable due to lack of follow-up. Physical evaluation of the siblings revealed OFCs of 47cm (<3%) and 44.3cm (<3%), respectively, delayed growth and developmental milestones, microcephaly, truncal hypotonia, and spasticity of lower extremities (Figure S1A). At examination, the patients were capable of supported sitting and smiling, and the eldest sibling was also able to crawl. Chromosome and sub-telomeric FISH analysis did not detect any aberrations. At the most recent evaluation, the parents had three additional children; two are unaffected. The youngest member of the family (BAB5318) was 6 months old, yet neither head support nor supported sitting had been achieved. Interestingly, this family was ascertained from our brain malformation cohort by correlating the facial features of patients from the HOU1338 and HOU1333 families (Figure 1). Brain MRI findings in three

affected siblings revealed microcephaly, decreased cortical volume and/or cortical atrophy (Figure 1). Vertical clivus was marked in BAB4770 and 5318, while mild in BAB4771 whose corpus callosum is comparatively mildly affected (Figure 1). BAB4771 also showed focal cerebellar vermis volume loss (Figure 1). Electrophysiological studies could not be performed since the parents refused.

Family HOU1380 presented to the Department of Neurology at Gaziantep Children`s Hospital due to seizures and developmental delay. Both patients were followed by several doctors with the diagnoses of cerebral palsy and epilepsy. BAB3519 is a female patient born following an uncomplicated pregnancy. The parents noticed floppiness at birth and tonic-clonic seizures starting on day 3 of the postnatal period. Mixed type (tonic, tonic-clonic and myoclonic) seizures were partially controlled by valproic acid. Denver development screening tests at 10 months of age revealed development consistent with 2 months of age. Anthropometric measurements at 10 month old were: W: 9 kg (50-75%), H: 71 cm (50-75%) and OFC: 39 cm (<3%), at 5 years, 4 months years old were W: 10.5 kg (<3%) and OFC: 42 cm (<3%) (Figure S1A). OFC measurement at 6 years, 5 months old was 42 cm (<3%) consistent with severe microcephaly (Figure S1A). Physical examination revealed severe DD/ID with no speech, rolling, babbling, or eye contact; increased DTRs; and hypertonicity of all four extremities. Facial dysmorphism including high arched eyebrow, long palpebral fissures, hypoplastic alae nasi, and retrognathia were similar to previous families (Figure 1). BAB3520, affected brother of BAB3519, was born after an uncomplicated pregnancy. Seizures started on day 51 after delivery and the family stated that neurodevelopment was always delayed compared to his peers. OFC measurements at 2 months old were: 37 cm (25-50%), at 3 years 9 month old was: 42 cm (<3%) and at 4 years 10

month old was 44 cm (<3%) (Figure S1A). Physical examination at age 3 years, 9 month was similar to BAB3519 with severe DD/ID, hypertonicity and increased DTRs. The same dysmorphic facial pattern was also noted in this patient (Figure 1). Seizures were mixed type and partially controlled with anti-epileptics. Cerebral imaging studies in both siblings revealed fronto-temporal atrophy most prominent in the temporal regions, thin corpus callosum and vertical clivus (Figure 1). In addition, BAB3520 also presented mild volume loss of inferior cerebellar vermis and mild thinning of the brain stem (Figure 1). Electrophysiological studies of both siblings were consistent with mild sensorimotor neuropathy (Figure 2 and Table S1).

Family HOU1981 was referred to Bezmialem University, Department of Medical Genetics because of psychomotor retardation, seizures and growth delay in both siblings at ages 3 and 1 year, 8 months (BAB4980 and 4981, respectively). Physical evaluation of both siblings revealed all anthropometric measures under the 3rd percentile, lack of speech and supportless sitting, truncal hypotonia with hypertonicity of lower extremities and exotropia of both eyes. Facial characteristics were similar with other patients (Figure 1). Brain MRI studies of both siblings showed evidence of microcephaly, generalized volume loss of cortex prominently affecting the fronto-temporal region, hypoplasia of the corpus callosum, delayed myelination, and vertical clivus (Figure 1). Electrophysiological studies studies demonstrated sensorimotor neuropathy (Figure 2 and Table S1A).

Overall all subjects share a similar pattern of clinical features including: i) severe global developmental delay, ii) abnormal tone, iii) microcephaly and brain dysgenesis, iv) seizures, and v) axonal sensorimotor neuropathy (Figures 1, 2 and S1A).

This study was approved by the Institutional Review Board of Baylor College of Medicine and informed consent was obtained from parents of all subjects.

Sanger PCR confirmation and segregation studies. To confirm the mutation detected by exome sequencing and to perform segregation analysis, standard PCR was carried out as previously described (Pehlivan et al., 2012) by using CLPF1: 5`-AGAGCTGACCCGAAACAAGA-3` and CLPR1: 5`-CCAGCTGAGAAAATGCAGTG-3` primers. Amplification products were electrophoresed on 0.8% agarose gels. PCR products were purified using ExoSAP-IT (Affymetrix, Santa Clara, CA) and analyzed by standard Sanger di-deoxy nucleotide sequencing (DNA Sequencing Core Facility at Baylor College of Medicine, Houston, TX).

OFC calculations. WHO head circumference data is only available from birth to age 5 years. Therefore, we used head circumference data from the literature for boys and girls starting from birth to 18 years (Roche et al., 1987). For time points that were not available in the primary data, we interpolated the values for both mean and standard deviation using the R statistical programing language (R Core Development Team).

Purification of recombinant GST-CLP1 proteins from *E. coli.* The open reading frames for human CLP1 wild type, K127A, or R140H mutant versions (obtained by PCR site-directed mutagenesis) were recombined into the pDEST15 plasmid using the Gateway system (Invitrogen), encoding an N-terminal glutathione *S*-transferase tag. Plasmids were then

transformed into *E. coli* (BL21-Codon Plus). An overnight culture of 100 ml in LB medium was diluted into 1.2 L of LB medium to OD_{600nm} = 0.1, and after further incubation until an OD_{600nm} = 0.4, CLP1 proteins were expressed for 2 hrs at 37°C by addition of 0.1 mM isopropyl β-D-thiogalactoside (IPTG; Fermentas, Thermo Scientific). Cells were harvested by centrifugation (4,000 rpm for 20 min) and the cell pellet re-suspended in 20 ml extraction buffer (50 mM Tris-HCl pH 8.0, 100 mM NaCl, 5 mM $MgCl_2$, 0.1% Tween-20, 1 mM DTT, 0.1 mM AEBSF). The cells were lysed by sonication and centrifuged at 16,000 rpm for 30 min. The supernatant was added to 1 ml equilibrated glutathione-Sepharose FF (GE Healthcare) and incubated on a rotating wheel for 2 hrs at 4°C. The resin was transferred to a chromatography column (BioRad), and washed with wash buffer (equals extraction buffer lacking Tween-20). GST-tagged proteins were eluted by incubating the resin with 1 ml of elution buffer (equals wash buffer plus 20 mM reduced Glutathione [Sigma]) for 10 min. Finally, the protein concentration was measured by Bradford (BioRad Bradford reagent). The total yield of recombinant CLP1 proteins recovered from 1.2 L bacterial culture was usually 0.3 mg.

Cell Culture. Phoenix, HEK293 cells and human fibroblasts were cultured at 37°C, 95% humidity and 5% CO_2 in Dulbecco's Modified Eagle's Medium (DMEM) supplemented with 10% fetal bovine serum, 3 mM glutamine, 100 U/ml penicillin and 100 μg/ml streptomycin sulfate (all reagents from Sigma). Cells were split and/or harvested using 0.05% Trypsin–EDTA.

Cell Extracts. For assaying biochemical activities using patient (BAB3401 and 3402) and parental (BAB3845 and 3846) fibroblasts, we prepared nuclear and cytoplasmic extracts. Cells from at least four confluent 15 cm dishes were trypsinized, the cell pellet washed once with PBS and spun for 2 min at 1,200 rpm. The pellet was re-suspended in 1 mL 1X PBS and transferred to a 1.5 mL tube. The tubes were centrifuged for 5 min at 1,200 rpm. The pellet was re-suspended

in one volume Buffer A (10 mM HEPES-KOH pH 8.0, 1 mM $MgCl_2$, 10 mM KCl, 1 mM DTT) and incubated for 15 min on ice. A 1-mL syringe (fitted with a 0.5 mm x 16 mm needle) was filled with Buffer A and thereafter fully displaced by the plunger to remove all the remaining air within the syringe. Cells were lysed by slowly drawing the suspension into the syringe followed by rapidly ejecting against the tube wall. This step was repeated four times for complete lysis to occur. The sample was then spun for 20 sec at 13,000 rpm and the post-nuclear supernatant (defined as cytoplasmic extract) was recovered. The pellet was re-suspended in two-thirds of one packed cell volume in Buffer C (20 mM HEPES-KOH pH 8.0, 1.5 mM $MgCl_2$, 25 % (v/v) glycerol, 420 mM NaCl, 0.2 mM EDTA, 0.1 mM PMSF, 1 mM DTT) and incubated on ice with stirring for 30 min. The suspension was centrifuged for 5 min at 12,000 rpm. For RNA kinase, tRNA splicing and RNA interstrand ligation assays, the supernatant (corresponding to nuclear extracts) was dialyzed for 1 hr against 30 mM HEPES-KOH pH 7.4, 100 mM KCl, 5 mM $MgCl_2$, 10 % (v/v) glycerol, 1 mM DTT, 0.1 mM AEBSF using dialysis membranes (Millipore 'V' series membrane). Afterwards, protein concentrations were determined (BioRad Bradford reagent), equalized using dialysis buffer and immediately used for enzymatic assays or snap-frozen and stored at -80°C.

Generation of stable cell lines expressing FLAG-CLP1 versions. The open reading frames for human CLP1 wild type, K127A, or R140H mutant versions were recombined into an in-house adapted version of the pBMN-GFP retroviral expression vector to allow gene shuttling using the Gateway system (Invitrogen) and expression as N-terminally FLAG-tagged proteins. Vectors were transfected into Phoenix packaging cell lines using conventional calcium-phosphate mediated transfection protocols. Supernatant medium containing retroviral particles were consecutively collected after 36 and 60 hours post-transfection, filtered and used to infect

HEK293 cells in the presence of 5 μg/mL polybrene (Millipore). Stably FLAG-CLP1 expressing cells were obtained after fluorescence activated cell sorting, propagated and subsequently used for affinity-purification of tagged CLP1 protein complexes.

Affinity purification of FLAG-CLP1 complexes. Confluent HEK293 cells from a 25x25 cm dish and stably expressing FLAG-tagged CLP1 wild type, K127A or R140H mutant versions (or not expressing any FLAG-tagged protein as control) were washed with PBS and harvested on ice by scraping with ice cold buffer P500 (30 mM Tris-HCl pH 7.5, 500 mM NaCl, 2 mM $MgCl_2$, 5 % (w/v) glycerol, 0.1 % (w/v), Triton X-100, 0.1 mM PMSF, 4 mM β-mercaptoethanol, supplemented with Phosphatase Inhibitor Cocktail Set II [Merck]). Cells were lysed by sonication and the extract cleared by centrifugation at 14,000 rpm for 30 min at 4°C. Tagged proteins were purified with anti-FLAG M2 affinity gel (Sigma) equilibrated in buffer P500 (40 μL of gel per confluent 25x25 cm dish). The resin was washed four times with buffer P500 and four times with buffer P100 (30 mM Tris- HCl pH 7.5, 100 mM NaCl, 2 mM $MgCl_2$, 5 % (w/v) glycerol, 0.1 % (w/v) Triton X-100, 4 mM β-mercaptoethanol). Affinity-purified FLAG-tagged proteins were eluted with buffer P100 supplemented with 2 mg/mL FLAG peptide by shaking in a Thermomixer for 30 min at 4°C.

Pre-tRNA cleavage and splicing assays. A PCR was performed using *S. cerevisiae* genomic DNA as template, a 5' primer including the T7 polymerase promoter (5'-AAT TTA ATA CGA CTC ACT ATA GGG GAT TTA GCT CAG TTG GG- 3'), and a 3' primer (5'-TGG TGG GAA TTC TGT GGA TCG AAC-3'). The PCR product was sequenced and identified as yeast tRNA3-Phe^{GAA} (chromosome 13). The PCR product served as template for *in vitro* transcription using the T7 MEGAshortscript kit (Ambion) including 1.11 MBq [α-^{32}P] guanosine-5'-triphosphate (111 TBq/mmol, Perkin Elmer) per reaction. The pre-tRNA was resolved in a 10 % denaturing

polyacrylamide gel containing 8 M urea (Sequagel, National Diagnostics), visualized by autoradiography and passively eluted from gel slices overnight in 0.3 M NaCl. RNA was precipitated by addition of three volumes of ethanol, and dissolved at 1 µM in buffer containing 30 mM HEPES-KOH pH 7.3, 2 mM $MgCl_2$, 100 mM KCl. To assess pre-tRNA cleavage or splicing, four volumes of reaction buffer (100 mM KCl, 5.75 mM $MgCl_2$, 2.5 mM DTT, 5 mM ATP, 6.1 mM Spermidine-HCl pH 8.0 (Sigma) and one volume of 1 µM body-labeled *S. cerevisiae* pre-$tRNA^{Phe}$ were mixed, heated at 95°C for 90 sec and incubated for 20 min at room temperature. RNasin RNase inhibitor (Promega) was added to a final concentration of 6 U/mL. Equal volumes of the described reaction mixture and affinity-purified FLAG-CLP1 complexes from stably expressing HEK293 cell lines obtained after elution with FLAG peptide, or cell extracts (cytoplasmic or nuclear) derived from parental and patient fibroblasts were mixed and incubated at 30°C. At given time points, 5 µL of the mix were deproteinized with Proteinase K, followed by phenol/chloroform extraction and ethanol precipitation. Reaction products were separated on a 10% denaturing polyacrylamide gel containing 8 M urea (Sequagel, National Diagnostics), and mature tRNA formation and/or tRNA exon formation was monitored by phosphorimaging.

RNA kinase assay and interstrand ligation assay. 50 pmol RNA oligonucleotide derived from the firefly luciferase gene (5'-UCG AAG UAU UCC GCG UAC GU-3', Dharmacon) were incubated with 1.11 MBq [5'-^{32}P] cytidine-3',5'-bisphosphate (111 TBq/mmol, Perkin Elmer) and 20 units T4 RNA ligase 1 (NEB) for 1 hr at 16°C in 15% (v/v) DMSO, 50 mM Tris-HCl pH 7.6, 10 mM $MgCl_2$, 10 mM β-mercaptoethanol, 200 µM ATP, 0.1 mg/mL BSA in a total reaction volume of 10 µL. Labeling reactions were resolved by denaturing gel electrophoresis in 15% polyacrylamide gels containing 8 M urea (SequaGel, National Diagnostics). The 3' end-labeled

RNA was visualized by autoradiography and passively eluted from gel slices overnight at 4°C in 0.3 M NaCl. The RNA was precipitated by adding three volumes of ethanol and for the RNA interstrand-ligation assay directly annealed to a non-labeled, complementary RNA oligonucleotide (5'-CGU ACG CGG AAU ACU UCG A-3', Dharmacon, Thermo Scientific) as described below. Alternatively, for the RNA kinase assay the 3' end-labeled RNA was first dephosphorylated (in a 120 µL reaction, 1 U Alkaline Phosphatase AP (Roche) and Roche-supplied buffer) for 30 min at 37°C. The reaction was then deproteinized by Proteinase K, followed by phenol/chloroform extraction and ethanol precipitation. The RNA was further annealed with a non-labeled complementary RNA oligonucleotide (5'-CAC GUA CGC GGA AUA CUU CGA-3', Dharmacon). Annealing reactions were performed as follows: 50 nM labeled and non-labeled complementary RNA oligonucleotide were mixed in 30 mM HEPES-KOH pH 7.5, 2 mM $MgCl_2$ and 100 mM KCl, heated to 95°C for 2 min and subsequently incubated at 37°C for 1 hr. The obtained RNA duplexes were directly used as substrates for the RNA interstrand ligation or RNA kinase assay.

The RNA kinase assay was performed by adding equal volumes of affinity-purified FLAG-CLP1 complexes from stably expressing HEK293 cell lines obtained after elution with FLAG peptide, or of cell extracts (cytoplasmic or nuclear) derived from parental and patient fibroblasts and reaction mixture (100 mM KCl, 5 mM $MgCl_2$, 10 mM DTT, 2 mM ATP, 0.4 mM GTP and 64 U/ml RNasin [Promega]) containing 10 nM radio-labeled RNA duplex, followed by incubation at 30°C. At given time points, 5 µL of the reaction was quenched by adding 5 µL of 8 M urea solution. Reaction products were separated on a 15 % denaturing acrylamide gel containing 8 M urea (Sequagel, National Diagnostics), and RNA phosphorylation was monitored by phosphorimaging. To test for RNA interstrand ligation, 3 µL reaction mixture (167 µM EDTA

pH 8.0, 67 mM KCl, 2 mM $MgCl_2$, 8.3 mM DTT, 5 mM ATP, 0.3 mM GTP, 53 U/mL RNasin (Promega), 43% glycerol) containing 17 nM radio-labeled RNA duplex were mixed with 2 μL nuclear fibroblast extracts and incubated for 30 min at 30°C. Reactions were deproteinized with Proteinase K, followed by phenol/chloroform extraction and ethanol precipitation. Reaction products were separated on a 15% denaturing polyacrylamide gel containing 8 M urea (Sequagel, National Diagnostics) and radiolabeled RNA was visualized by phosphorimaging.

Northern blot analyses. Isolation of total RNA from patient (BAB3401 and 3402) or parental (BAB3845 and 3846) fibroblasts was performed using the Trizol Reagent (Invitrogen) according to the manufacturer's instructions. Typically 4-5 μg of RNA was separated in a 10% (or in case for Northerns to detect tRNA introns, in a 15 %) denaturing polyacrylamide gel (20 x 25 cm; Sequagel, National Diagnostics). The RNA was blotted on Hybond-N+ membranes (GE Healthcare) and fixed by ultraviolet cross-linking. Membranes were pre-hybridized in 5X SSC, 20 mM Na_2HPO_4 pH 7.2, 7 % SDS, 1X Denhardt's solution and 0.1 mg/mL sonicated salmon sperm DNA (Stratagene) for 1 hr at 80° C (for DNA/LNA probes) or 50°C (for DNA probes). Hybridization was performed in the same buffer overnight at 80°C (for DNA/LNA probes) or 50°C (for DNA probes) including 100 pmol of the following [5'-^{32}P]labeled DNA/LNA probes (Exiqon, Denmark; LNA nucleotides are indicated by "*X"): tyrosine tRNA-GTA 5' exon probe, 5'-CT*A CA*G TC*C TC*C GC*T CT*A CC-3'; tyrosine tRNA-GTA exon junction probe, 5'-AC*C TA*A GG*A TC*T AC*A GT*C CT-3'; isoleucine tRNA-TAT 5' exon probe, 5'-TA*T AA*G TA*C CG*C GC*G CT*A AC-3', or following DNA probes: methionine 5' tRNA-CAT probe, 5'-GGG CCC AGC ACG CTT CCG CTG CGC CAC TCT GC-3'; leucine tRNA-CAA 5' exon probe, 5'-CTT GAG TCT GGC GCC TTA GAC-3'; isoleucine tRNA-TAT intron probe (Chr2.trna5-IleTAT), 5'-TGC TCT GCA TGT ACT GCT G-3'; isoleucine tRNA-TAT intron

probe (Chr19.trna10-IleTAT), 5'-TGC TCC GCT CGC ACT GTC A-3'; tyrosine-GTA intron probe (Chr2.tRNA2-TyrGTA), 5'-TTG CCA CGC CCT ATC CAC TA-3'; tyrosine-GTA intron probe (Chr8.tRNA4-TyrGTA), 5'-GTC TCC TGC TGA GGA AGT AG-3'; tyrosine-GTA intron probe (Chr6.tRNA14-TyrGTA), 5'-GTC TAA GGA CAC AGC CAA-3'; arginine tRNA-TCT 5' exon probe, 5' TAG AAG TCC AAT GCG CTA TCC; arginine-TCT intron probe (Chr17.tRNA4-ArgTCT), 5'-ATT GCT CTA TTC GTC ACT AG-3'; arginine-TCT intron probe (Chr1.tRNA9-ArgTCT), 5'-GAA TGC CTT CAG CCT CTA GA-3'. Subsequently blots were washed twice for 1 min at 50°C with 5X SSC, 5% SDS and once for 1 min with 1X SSC, 1% SDS and analyzed by phosphorimaging. Membranes were re-hybridized at 50°C using a DNA probe (5'-GCA GGG GCC ATG CTA ATC TTC TCT GTA TCG-3') complementary to U6 snRNA to check for equal loading.

tRNA deep sequencing. Total RNA was isolated from patient (BAB3401 and 3402) or parental (BAB3845 and 3846) fibroblasts using the TRIzol Reagent (Invitrogen) according to the manufacturer's instructions. For each sample 300 ng of total RNA were hydrolyzed in a 15 µL buffer of 10 mM Na_2CO_3 and 10 mM $NaHCO_3$ at pH 9.7, for 5 minutes at 90°C. The hydrolyzed RNA was dephosphorylated with 10 U of calf intestinal phosphatase (NEB) in a 50 µL reaction of 100 mM NaCl, 50 mM Tris-HCl pH 7.9 at 25°C, and 10 mM $MgCl_2$, 1 mM DTT, 3 mM Na_2CO_3 and 3 mM $NaHCO_3$, at 37°C for 1 h. The resulting RNA was re-phosphorylated with 10 U of T4 polynucleotide kinase (NEB) in a 20 µl reaction of 70 mM Tris-HCl pH 7.6 at 25°C, and 10 mM $MgCl_2$, 5 mM DTT and 1 mM ATP, at 37°C for 1 h. Fragments of 19-24 nts were converted into barcoded small RNA cDNA libraries, as previously described (Hafner et al., 2012), and submitted for Illumina sequencing. Sequencing read alignments were performed using the Burrows-Wheeler aligner against an in-house curated and annotated list of mature and

precursor tRNAs (Li and Durbin, 2009). Sequencing reads were first mapped against mature tRNAs. Remaining reads were mapped against genomic tRNA sequences that included 5' leader and 3' trailer sequences, as well as tRNA introns.

Basic structural properties and modification analysis of tRNA introns. 70 µg of total RNA from fibroblasts derived from patient BAB3401 was separated alongside with a radiolabeled RNA decade marker (Ambion) on a preparative 10% denaturing polyacrylamide gel (20 × 25 cm, 1 mm thick) containing 8 M urea (Sequagel, National Diagnostics). The gel region comprising sizes of 15-25 nucleotides was excised and passively eluted overnight into 0.4 M NaCl. The RNA was precipitated by adding three volumes of ethanol, the pellet was washed once in 85% ethanol and dissolved in H_2O (intron-containing RNA). A 5' OH-terminating synthetic RNA (IBA Lifesciences) composed of the intronic sequence of tRNA-Ile-TAT (Chr19.trna10; 5' OH-UGA CAG UGC GAG CGG AGC A-3') served as control. To obtain circular control RNA, synthetic intron RNA was 5' phosphorylated with T4 PNK/ATP, subsequently deproteinized, extracted with phenol/chloroform, precipitated with ethanol and dissolved in H_2O. Circularization was performed by treatment with T4 RNA Ligase I (NEB) including 15% polyethylene glycol 8000 on ice overnight.

For basic structural analysis, an aliquot of linear and circular control RNAs, and patient intron-containing RNA was left untreated or incubated for 1 h at 37°C with RNase R (Epicentre) according to the manufacturer's instruction. For assessing the 5' end modification of intronic patient RNA, an aliquot of linear and circular control RNA, and patient intron-containing RNA was left untreated or 5´ phosphorylated with T4 PNK/ATP (or recombinant CLP1/ATP), deproteinized, extracted with phenol/chloroform, precipitated with ethanol and dissolved in H_2O. Aliquots of RNA were either left untreated or incubated with a synthetic RNA 32-mer linker (5' OH-GCU GAC CCU GAA GUU CAU CUG CAC CAC CGG CA-OH 3') and T4 RNA Ligase I (NEB) including 15% polyethylene glycol

8000 on ice overnight. All reaction products were subsequently subjected to Northern blotting and detected with a DNA probe complementary to the isoleucine tRNA-TAT intron (Chr19.trna10).

Western blotting. Western blot was carried out with antibodies reactive to FLAG peptide (anti-FLAG M2, Sigma), CLP1 (anti-HEAB, Abcam), β-actin (Sigma), and RAD50 (Abcam). In addition, rabbit polyclonal antibodies (Gramsch Laboratories, Schwabhausen, Germany) were raised against peptides of human TSEN2 (N-NGDSGKSGGVGDPREPLG-C), TSEN34 (N-AKKQKLEQASGASSSQEAGS-C), TSEN54 (N-RSRSQKLPQRSHGPKDFLPD-C), and HSPC117 (N-RHGAGRALSRAKSRRNLD-C). Sera were affinity-purified. Proteins were separated by SDS–PAGE, transferred to Immobilon-P membranes (Millipore) and probed with the antibodies described above using standard protocols.

Supplementary Figures

Supplementary Figure 1. Head circumference analysis of patients, and full pedigrees with sanger sequencing results of the families, Refers to Figure 1.

(A) Top. The mean and ± 2 standard deviation reference values for fronto-occipital circumference are plotted as solid and dotted black lines, respectively, for both males and females. Each patient's head size over time is also presented as a different color line. In the case where only one accurate data point was available, the measurement is indicated as a colored point. **Bottom**. Z scores, defined as the number of standard deviations the patient's head size deviates from the mean reference, for each time point are presented as a line or point of matching color. **(B)** Full pedigrees with sanger sequencing results of the families showing that R140H mutation co-segregates with the disease phenotype in all families, with each heterozygous parent contributing a variant allele in accordance with Mendelian expectations.

Supplementary Figure 2. Western and Northern blot analyses on patient fibroblasts, Refers to Figure 4-5.

(A) RNA ligation assay of nuclear extracts from parental and patient fibroblasts incubated with an RNA duplex bearing 5' OH groups and a [^{32}P]Cp 3'end-label. Interstrand ligation by the tRNA ligase activity of the HSPC117 complex was monitored by denaturing gel electrophoresis. The panel is a representative example of triplicate experiments. **(B, C)** Western blot analysis to confirm presence of CLP1 and components of the tRNA splicing pathway in nuclear **(B)** and cytoplasmic **(C)** extracts used in the assays shown in Figure 4F-H and Figure S2A. **(D)** Northern blot analyses of RNA from parental (BAB3845 and 3846) and patient (BAB3401 and 3402) fibroblasts. Pan-probes were used to detect multiple tRNA species at once or to cover tRNAs of the same isotype. A pan-probe directed against the tRNA 5' region was used to detect mature levels of intron-less methionine-CAT tRNAs. A pan-probe specifically designed to detect the exon junction region was used to detect mature levels of intron-encoding tyrosine-GTA tRNAs. In order to assess pre- and mature levels of intron-encoding leucine-CAA and arginine-TCT tRNAs, pan-probes complementary to the 5' exon regions were used. U6 snRNA served as loading control. **(E)** Northern blot analyses of RNA from parental (BAB3845 and 3846) and patient (BAB3401 and 3402) fibroblasts to specifically detect pre-tRNAs of indicated intron-

encoding tRNAs using probes directed against the intronic regions. Asterisks denote truncated pre-tRNA species. U6 snRNA served as loading control. **(F,G)** Quantification of mature and pre-tRNA levels. Mature and pre-tRNA signal intensities from Northern blots described in Figure 5A-C and Figure S2D-E were quantified using the ImageQuant TL (GE Healthcare) software and standardized to corresponding U6 snRNA intensities. Values represent relative signal intensities. The highest signal intensity for the detection by a given tRNA probe was arbitrarily set to 1.0.

Supplementary Figure 3. Quantification and biochemical characterization of tRNA introns, Refers to Figure 5.

(A) tRNA intron signal intensities from Northern blots described in Figure 5A-C were quantified using the ImageQuant TL (GE Healthcare) software and standardized to corresponding U6 snRNA intensities. Values in the Table (upper panel) represent relative signal intensities. The highest signal intensity for the detection by a given tRNA probe was arbitrarily set to 1.0. Lower panel shows a graphical representation of values. **(B)** Quantification of tRNA intron read counts (mapping fully within introns) obtained from deep sequencing of RNA derived from parental and patient fibroblasts. Values in the upper panel represent relative read counts. Normalization was performed over median precursor tRNA read counts. The highest read count value for a given tRNA species was arbitrarily set to 1.0. Lower panel shows a graphical representation of values in the upper panel. **(C**) Alignment of RNA-seq reads from parental (BAB3846, left panel) and patient (BAB3402, right panel) fibroblasts against precursor isoleucine-TAT (Chr19.tRNA10). Total RNA was subjected to partial alkaline hydrolysis prior to cloning and sequencing. Reads were aligned against an in-house curated list of mature and pre-tRNAs. The mature tRNA (blue), the tRNA intron (orange), and the 5' leader and 3' trailer sequences (green) are shown for each tRNA. The frequency of each read is also presented (count). All reads mapped uniquely to the identified positions. Reads that lie completely within the intron are depicted in orange, reads that span the intron/exon junction in orange/blue and reads that span the mature/precursor border in blue/green. Upstream and downstream nucleotides with no sequencing evidence are shown in black. Vertical lines represent the relative frequency of binned, normalized read counts in $\log_2$ increments. **(D-E)** tRNA introns derived from isoleucine-TAT (Chr19.tRNA10) in patient

fibroblasts are linear and display a 5' hydroxy group. Total RNA from fibroblasts derived from patient BAB3401 was size-fractionated by gel electrophoresis and the RNA pool comprising 15-25 nucleotides was isolated (containing tRNA introns). A linear 5' OH group (19-mer) terminating or a circular (19-mer and 38-mer) synthetic RNA comprising the Ile-TAT (Chr19.tRNA10) sequence served as control. **(D)** Circular (left panel), linear (middle panel), and tRNA intron-containing RNA (right panel) was treated with RNase R which digests specifically linear but not circular or lariat RNA. Reaction products were subjected to Northern blotting and detected with a DNA probe complementary to the isoleucine tRNA-TAT intron (Chr19.trna10) sequence. tRNA intron as well as linear control RNA, but not circular control RNA, were digested by RNase R treatment, indicating that isoleucine tRNA-TAT introns (Chr19.trna10) accumulating in patient fibroblasts are linear. **(E)** Circular control RNA (left panel) and linear control (middle panel) and patient intron-containing RNA samples (right panel) were left untreated or 5´ phosphorylated with T4 PNK/ATP or recombinant CLP1/ATP. Subsequently RNA samples were either left untreated or incubated with a synthetic RNA 32-mer linker containing a 3' hydroxy group and T4 RNA Ligase I (ligation by T4 RNA Ligase I requires a 5' P group). All reaction products were subjected to Northern blotting and detected with a DNA probe complementary to the isoleucine tRNA-TAT intron (Chr19.trna10) sequence. Introns (and 5' hydroxy group terminating control 19-mer RNA) can only be ligated to the RNA linker upon prior 5' phosphorylation giving rise to a 51-mer ligation product, indicating that isoleucine tRNA-TAT introns (Chr19.trna10) accumulating in patient fibroblasts display a 5' hydroxy group.

Supplementary Figure 4. Microcephaly in viable *Clp1*$^{K/K}$ mutant mice, Refers to Figure 6.

(A) Brain weights of individual wild type *Clp1*$^{+/+}$ control and *Clp1*$^{K/K}$ littermates on a viable CBA/J background are shown (4-14 months old). Black lines in the graphs indicate means. (**B)** MRI measurements showing brain volumes (mm^3) and **(C)** brain aspect ratios (au) of 4, 8, and 12 weeks old *Clp1*$^{+/+}$ and *Clp1*$^{K/K}$ littermates. **(D)** MRI cortical thickness surface mapping of 28 weeks old *Clp1*$^{+/+}$ control and *Clp1*$^{K/K}$ littermates. The cortexes are colour-coded from dark blue to red to illustrate cortical thickness from 0 to 2.5 mm (see scale in Figure 6B). (**E**) Neocortex areas. The areas occupied by the six-layered neocortex were measured using coronal sections.

Graphs show data from individual *Clp1*$^{+/+}$ and *Clp1*$^{K/K}$ littermate mice. Black lines in the graphs indicate means. **(F)** Representative coronal H&E sections of *Clp1*$^{+/+}$ and littermate *Clp1*$^{K/K}$ mutant brains at eight months of age. Of note, there were no apparent focal lesions, haemorrhages, prominent gliosis, or detectable necrotic areas. Scale bars: 500 µm . * $P < 0.05$. *** $P < 0.001$.

Supplementary Figure 5. Cortex and cerebellar morphology in adult *Clp1*$^{K/K}$ mice, Refers to Figure 6.

(A) Histological (H&E staining) and immunohistochemical analysis with antibodies against NeuN to detect neurons in the brain of *Clp1*$^{+/+}$, *Clp1*$^{K/K}$, and *Clp1*$^{K/+}$ mice. Motor and sensory cortexes are shown above the hippocampus from 3-4 months old littermate mice on a CBA/J background. Scale bars: 500 µm. **(B,C)** Immunohistochemical analysis with antibodies to ionized calcium binding adaptor molecule 1 (Iba-1) to detect microglia in the neocortex of *Clp1*$^{+/+}$ and *Clp1*$^{K/K}$ mice. **(B)** Representative images of NeuN^{+} neurons and counterstaining with Hoechst 33342 (blue). Scale bars: 50 µm. Insets 10 µm. **(C)** Quantification (mean values +/- SEM) of Iba^{+} microglia in the neocortex. n = 6 mice per genotype. **(D,E)** Immunohistochemical analysis with antibodies to glial fibrillary-acidic protein (GFAP) to detect astrocytes in the hippocampus of *Clp1*$^{+/+}$ and *Clp1*$^{K/K}$ mice. Dentate gyrus and the CA1 region are shown from 3-4 months old littermate mice on a CBA/J background. **(D)** Representative images of GFAP^{+} astrocytes and counterstaining with Hoechst 33342 (blue). Scale bars: 50 µm. Insets 10 µm. **(E)** Quantification (mean values +/- SEM) of Iba^{+} microglia in the dentate gyrus and CA1 regions. n = 6 mice per genotype. **(F)** Sagittal cerebellar H&E sections of 8 months old *Clp1*$^{+/+}$ and *Clp1*$^{K/K}$ mutant mice. Scale bars: 500 µm. **(G)** Immunohistochemical analysis with antibodies against NeuN to detect neurons in the cerebella of *Clp1*$^{+/+}$ and *Clp1*$^{K/K}$ mice. Sections were counterstained with Hoechst 33342 to visualize nuclei. Data are from 3-4 months old littermates on a CBA/J background. Scale bars: 50 µm. **(H,I)** Immunohistochemical analysis with antibodies to GFAP to detect astrocytes (green) and Calbindin as a marker for cerebellar Purkinje cells (red) of 12 weeks old *Clp1*$^{+/+}$ and *Clp1*$^{K/K}$ mice on a CBA/J background. Note regular layering with intact Purkinje cells and no signs of astrogliosis. Scale bars: 100 µm in (H) and 25 µm in (I). **(J)** Quantification (mean values +/- SEM) of Calbindin^{+} Purkinje cells in the cerebella of *Clp1*$^{+/+}$

and *Clp1*$^{K/K}$ mice on a CBA/J background. Of note, Calbindin^{+} Purkinje cells were counted along the border between the molecular and granullar layers, i.e. where the cell bodies of Purkinje cells are localized, and are therefore given as cell numbers/mm. n = 4 mice per genotype. N.S. statistically not significant.

Supplementary Figure 6. Microcephaly in C57BL/6 *Clp1*$^{K/K}$ mutant embryos, Refers to Figure 7.

(**A**) Coronal H&E sections of *Clp1*$^{+/+}$ and *Clp1*$^{K/K}$ littermate embryo brains at E18.5. Scale bars: 500μm. (**B**) Representative sagittal H&E sections of *Clp1*$^{+/+}$ and *Clp1*$^{K/K}$ littermate embryos at E18.5. Note markedly reduced brain size in the *Clp1*$^{K/K}$ embryos. Scale bars: 1 mm. (**C**) Representative sagittal H&E sections of *Clp1*$^{+/+}$ and *Clp1*$^{K/K}$ littermate embryos at E18.5. Black boxes indicate the magnified regions to demonstrate reduction of the neocortex in the E18.5 *Clp1*$^{K/K}$ littermate. Scale bars: 200 μm. (**D**) Representative MRI images (7 Tesla MRI) of E16.5 (left panels) and E18.5 (right panels) *Clp1*$^{+/+}$ and *Clp1*$^{K/K}$ littermate embryos. Arrows indicate caudal-rostral and dorsal-ventral dimensions; values are given in cm. Scale bars: 200 μm. (**E**) Quantification of bulbus, cortex, and cerebellum volumes as determined via 15.2 MRI. Mean values +/- SEM are shown for E18.5 *Clp1*$^{+/+}$ and *Clp1*$^{K/K}$ littermate mice. n = 8 mice per genotype. (**F,G**) Analysis of brain geometries as determined by 15.2 MRI imaging. **(F)** Principal Component (PC) analyses for brain major PC (first PC - anterior-posterior direction, given in mm), brain minor PC (second PC - caudal-rostral direction, given in mm), and brain third PC (dorso-ventral direction, given in mm) and **(G)** cortical roundness (shown in arbitrary units) in E16.5 and E18.5 *Clp1*$^{+/+}$ and *Clp1*$^{K/K}$ littermate embryos. Data are shown as mean values +/- SEM. n = 8 mice per genotype. (**H**) Quantification (mean values +/- SEM) of Tbr1^{+} neuron numbers in the neocortex of *Clp1*$^{+/+}$ control and *Clp1*$^{K/K}$ E16.5 embryos on the neonatal lethal B6 background. Of note, the area of Tbr1^{+} cells encompasses the region from the lateral ventricle to the brain surface (width of 300 pixels, ~ 100 μm). n = 8 mice per genotype. * $P < 0.05$. ** $P < 0.01$. *** $P < 0.001$. N.S. statistically not significant.

Supplementary Figure 7. Immunostaining for Iba1, GFAP, Tbr1, Pax6, or Ki67 in C57BL/6 embryos, Refers to Figure 7.

(**A**) Immunohistochemical analysis with antibodies to Iba-1 to detect microglia in the neocortex of E16.5 and E18.5 *Clp1*$^{+/+}$ and *Clp1*$^{K/K}$ embryos on the B6 background. Sections were counterstained with Hoechst 33342 to visualize nuclei. Scale bars: 100 μm. Insets 25 μm. (**B**) Quantification (mean values +/- SEM) of Iba1^{+} microglia numbers in the neocortex. N.S. statistically not significant. (**C**) Representative images of immunostaining for GFAP in the indusium griseum, ventricular zone, or subventricular zone of E16.5 and E18.5 *Clp1*$^{+/+}$ and *Clp1*$^{K/K}$ embryos on the B6 background. Of note, due to the shape of the GFAP^{+} cells, we were not able to accurately assess cell numbers and thus can only present the images to show apparently normal distributions. Sections were counterstained with Hoechst 33342 to visualize nuclei. Scale bars: 50 μm. (**D,E**) Representative immunostainings for the neuronal progenitor marker Pax6 in the ventricular zone of *Clp1*$^{+/+}$ and *Clp1*$^{K/K}$ E16.5 and E18.5 embryos. Scale bars: in (D) 100 μm, and in (E) 50 μm. (**F**) Quantification (mean values +/- SEM) of Pax6^{+} neuronal progenitor cell numbers in the ventricular zone of E16.5 and E18.5 *Clp1*$^{+/+}$ control and *Clp1*$^{K/K}$ embryonic brains. Of note, the area of Pax6^{+} cells encompasses the region from the lateral ventricle to the brain surface (width of 300 pixels, ~ 100 μm). (**G**) Quantification (mean values +/- SEM) of Ki67^{+} proliferating cells in coronal sections of *Clp1*$^{+/+}$ and *Clp1*$^{K/K}$ E16.5 and E18.5 embryonic brains. N.S. statistically not significant.

Supplementary Table 1. Electrophysiological studies show evidence for axonal motor and sensory peripheral neuropathy, Refers to Figure 2.

Supplementary Table 2. tRNA deep sequencing evaluating mature tRNA levels in parental and patient fibroblasts. Refers to Figure 5 and Figure S2.

Total RNA of parental (BAB3845 and 3846) and patient (BAB3401 and 3402) fibroblasts was subjected to an RNA cloning protocol followed by deep sequencing. In order to overcome known problems of cloning and sequencing of highly structured and modified tRNAs, we applied a partial alkaline hydrolysis step of total RNA prior to adapter ligation and sequencing. Sequencing reads were aligned to an in-house annotated and curated list of precursor and mature tRNAs. All alignments were performed in a hierarchical fashion. First, all reads were aligned against the list of all mature tRNAs (including sequence variants resulting from nucleoside modifications). Subsequently the remaining reads were aligned against tRNA genomic loci for which RNA-seq evidence of expression is documented. This step included, thus, only reads that spanned the borders between the tRNA termini and the 5' leader or 3' trailer, as well as reads that mapped to introns of intron-containing tRNAs. Reads mapping to mature tRNAs of all intron-containing tRNAs (Leu, Arg, Tyr, Ile) and an intron-less tRNA (Met) were analyzed (**Sheet 1**). Read counts were normalized in each case against two metrics: the read count of a) the maximally expressed mature tRNA, b) the median mature tRNA. Parental and patient samples were averaged and enrichment ratios were obtained. tRNA sequences that were used for normalization are denoted in **Sheet 2**. Data have been deposited at the Gene Expression Omnibus (GEO). All primary data can be accessed using the link (http://www.ncbi.nlm.nih.gov/geo/query/acc.cgi?acc=GSE53391).

Supplementary Table 3. Results from tRNA deep sequencing evaluating intron tRNA levels in parental and patient fibroblasts. Refers to Figure S3.

Experimental procedure was as in Supplementary Table S2. All intron-containing tRNAs were examined by tallying the number of reads that mapped fully within introns (**Sheet 1**). Read counts were normalized in each case against four metrics: the read count of a) the maximally expressed mature tRNA, b) the median mature tRNA, c) the maximally expressed precursor tRNA, and d) the median precursor tRNA. Parental and patient samples were averaged and enrichment ratios were obtained. tRNA sequences that were used for normalization are denoted in **Sheet 2**. Data have been deposited at the Gene Expression Omnibus (GEO). All primary data can be accessed using the link (http://www.ncbi.nlm.nih.gov/geo/query/acc.cgi?acc=GSE53391).

Patient	BAB3401		BAB3402		BAB3421		BAB3422		BAB3519		BAB3520		BAB4980		BAB4981	
Age at Examination	8 years		6 years		8 years		6 years		7 years		5 years		2 Years		3 Years	
Sensory	Vel (m/s)	Amp (µV)	Vel (m/s)	Amp (µV)	Vel (m/s)	Amp (µV)	Vel (m/s)	Amp (µV)	Vel (m/s)	Amp (µV)	Vel (m/s)	Amp (µV)	Vel (m/s)	Amp (µV)	Vel (m/s)	Amp (µV)
R. Median	44	3.1	39.3	1.6	NR	NR	NR	NR	-	-	-	-	41.7	25.2	44.4	4.9
R. Ulnar	38.6	2	NR	NR	-	-	-	-	33.3	4.7	34.8	1.5	-	-	-	-
R. Sural	NR	NR	NR	NR	-	-	-	-	39.8	18	32.8	2.5	29.7	6.4	27.5	5.7
Motor	Vel (m/s)	Amp (mV)	Vel (m/s)	Amp (mV)	Vel (m/s)	Amp (mV)	Vel (m/s)	Amp (mV)	Vel (m/s)	Amp (mV)	Vel (m/s)	Amp (mV)	Vel (m/s)	Amp (mV)	Vel (m/s)	Amp (mV)
R. Median	39.3	2.8	36.2	4.3	41.2	1	40.3	1.1	-	-	-	-	45.9	2.3	40.9	4.2
R. C. Peroneal	37.3	0.4	28.4	1.4	42.5	1.1	39.8	1	41	4	40.5	7.4	47.6	3	47.2	1.64
R. Tibial	34.7	6.2	29.3	0.6	36.6	2.1	37.4	1.8	41.7	11.3	40.5	19.6	49	6.4	41.8	3.6

Vel, velocity; Amp, amplitude; R, right; -, not available; NR, non-recordable; C, common.

Supplementary Table 1

A

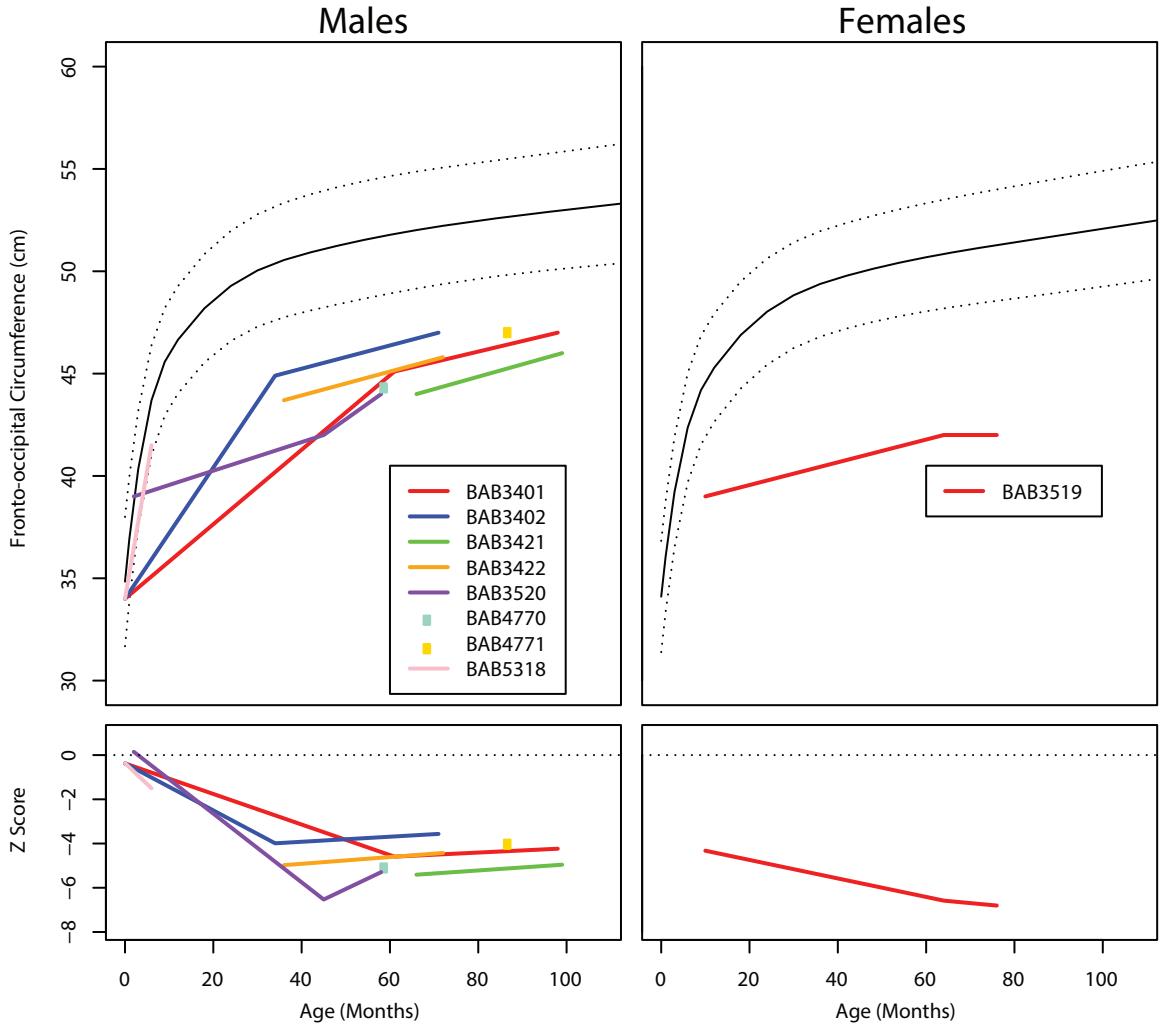

B

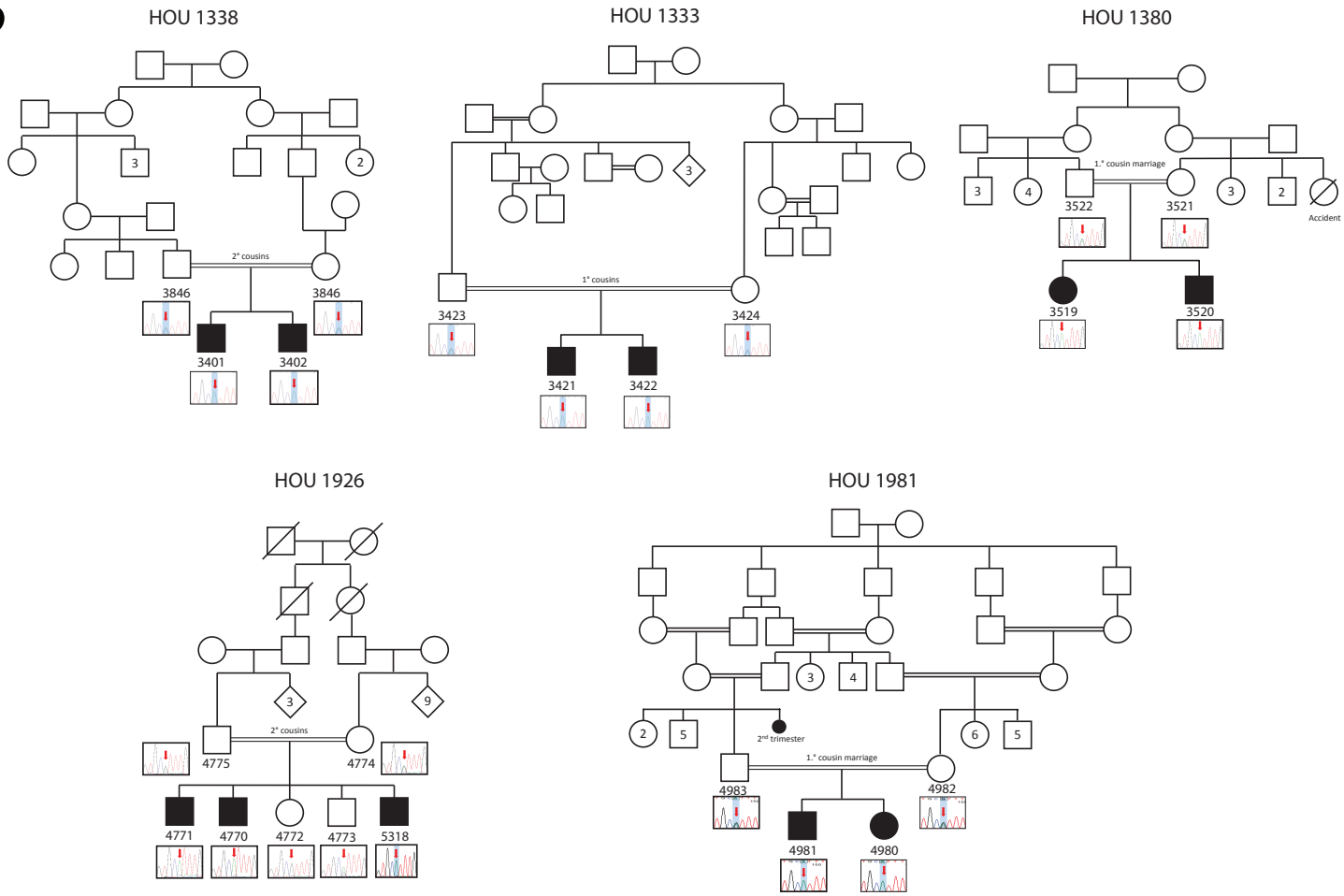

Supplementary Figure 1

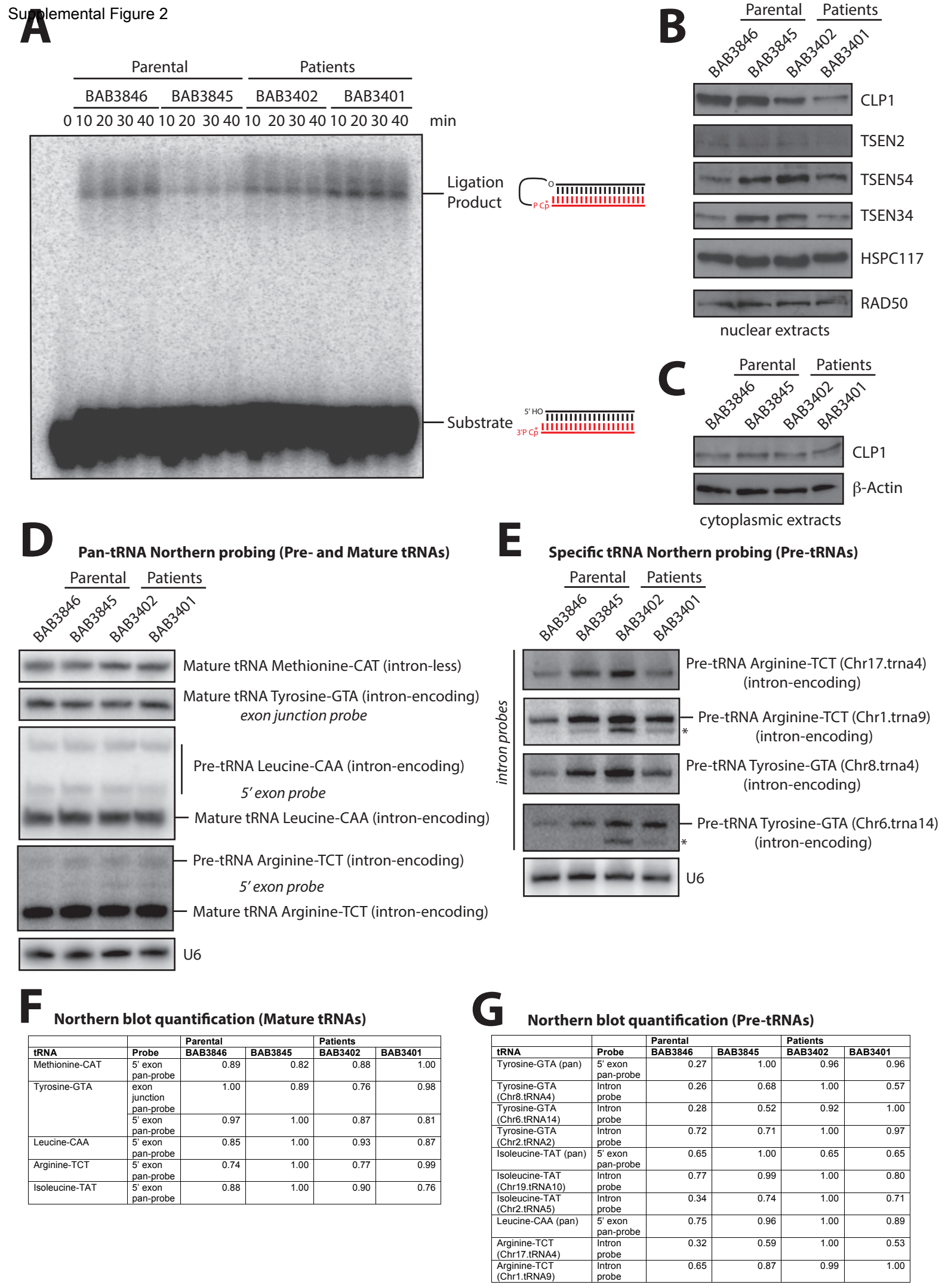

F Northern blot quantification (Mature tRNAs)

		Parental		Patients	
tRNA	Probe	BAB3846	BAB3845	BAB3402	BAB3401
Methionine-CAT	5' exon pan-probe	0.89	0.82	0.88	1.00
Tyrosine-GTA	exon junction pan-probe	1.00	0.89	0.76	0.98
	5' exon pan-probe	0.97	1.00	0.87	0.81
Leucine-CAA	5' exon pan-probe	0.85	1.00	0.93	0.87
Arginine-TCT	5' exon pan-probe	0.74	1.00	0.77	0.99
Isoleucine-TAT	5' exon pan-probe	0.88	1.00	0.90	0.76

G Northern blot quantification (Pre-tRNAs)

		Parental		Patients	
tRNA	Probe	BAB3846	BAB3845	BAB3402	BAB3401
Tyrosine-GTA (pan)	5' exon pan-probe	0.27	1.00	0.96	0.96
Tyrosine-GTA (Chr8.tRNA4)	Intron probe	0.26	0.68	1.00	0.57
Tyrosine-GTA (Chr6.tRNA14)	Intron probe	0.28	0.52	0.92	1.00
Tyrosine-GTA (Chr2.tRNA2)	Intron probe	0.72	0.71	1.00	0.97
Isoleucine-TAT (pan)	5' exon pan-probe	0.65	1.00	0.65	0.65
Isoleucine-TAT (Chr19.tRNA10)	Intron probe	0.77	0.99	1.00	0.80
Isoleucine-TAT (Chr2.tRNA5)	Intron probe	0.34	0.74	1.00	0.71
Leucine-CAA (pan)	5' exon pan-probe	0.75	0.96	1.00	0.89
Arginine-TCT (Chr17.tRNA4)	Intron probe	0.32	0.59	1.00	0.53
Arginine-TCT (Chr1.tRNA9)	Intron probe	0.65	0.87	0.99	1.00

Supplementary Figure 2

Supplemental Figure 3

A

Northern analysis
(normalized over U6 snRNA)

		Parental		Patients	
tRNA	Probe	BAB3846	BAB3845	BAB3402	BAB3401
Isoleucine-TAT (Chr19.tRNA10)	Intron probe	0.09	0.15	1.00	0.92
Isoleucine-TAT (Chr2.tRNA5)	Intron probe	0.02	0.03	1.00	0.76
Tyrosine-GTA (Chr2.tRNA2)	Intron probe	0.03	0.05	0.92	1.00

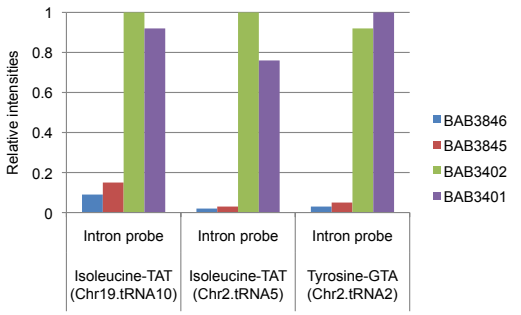

B

Deep sequencing analysis
(normalized over median precursor tRNA)

	Parental		Patients	
tRNA	BAB3846	BAB3845	BAB3402	BAB3401
Isoleucine-TAT (Chr19.tRNA10)	0.22	0.20	1.00	0.85
Isoleucine-TAT (Chr2.tRNA5)	0.10	0.11	1.00	0.39
Tyrosine-GTA (Chr2.tRNA2)	0.05	0.09	0.43	1.00

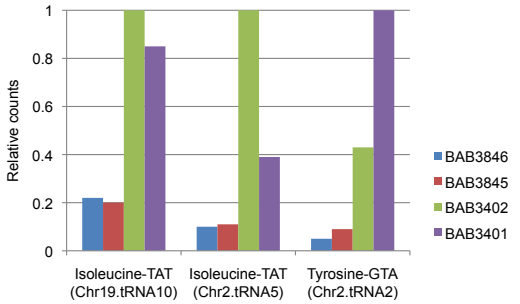

C

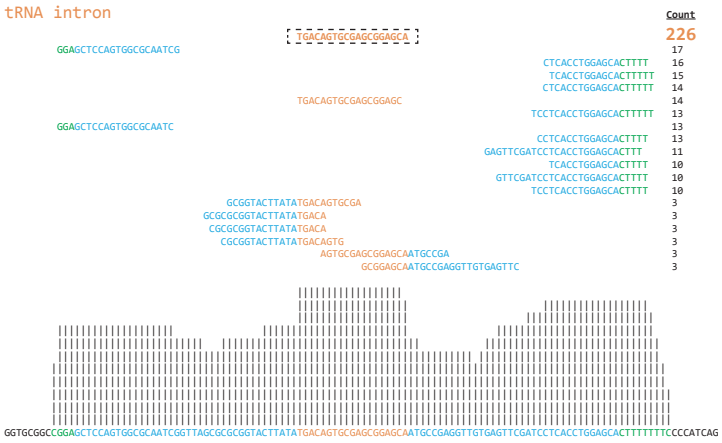

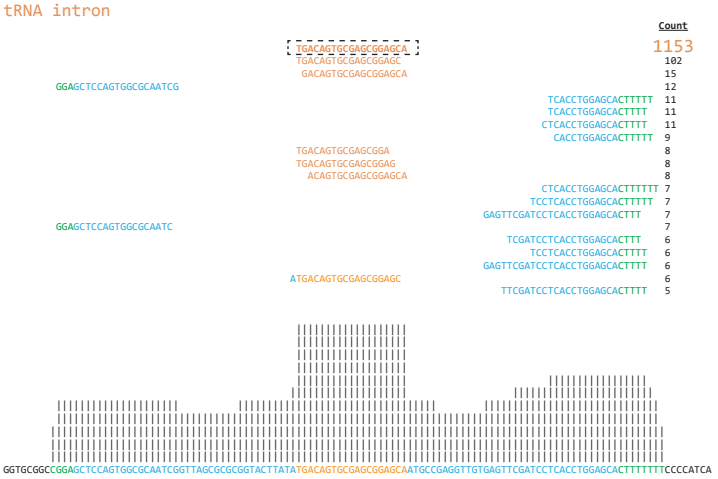

D

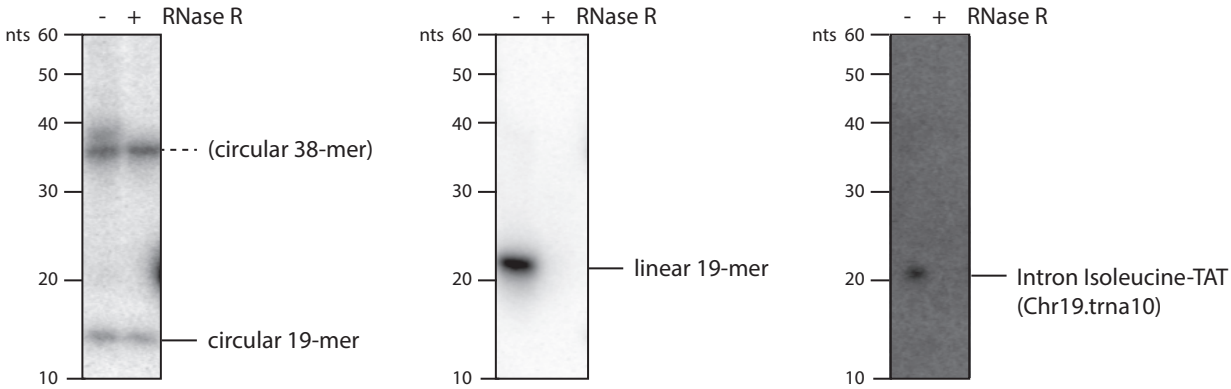

E

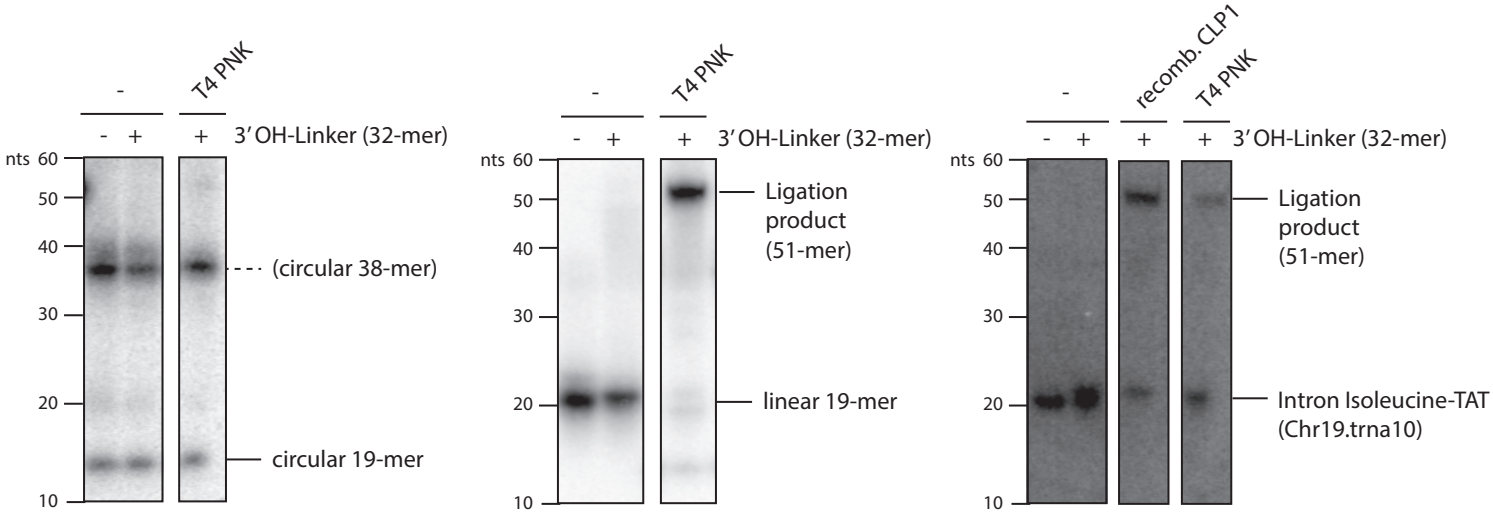

Supplementary Figure 3

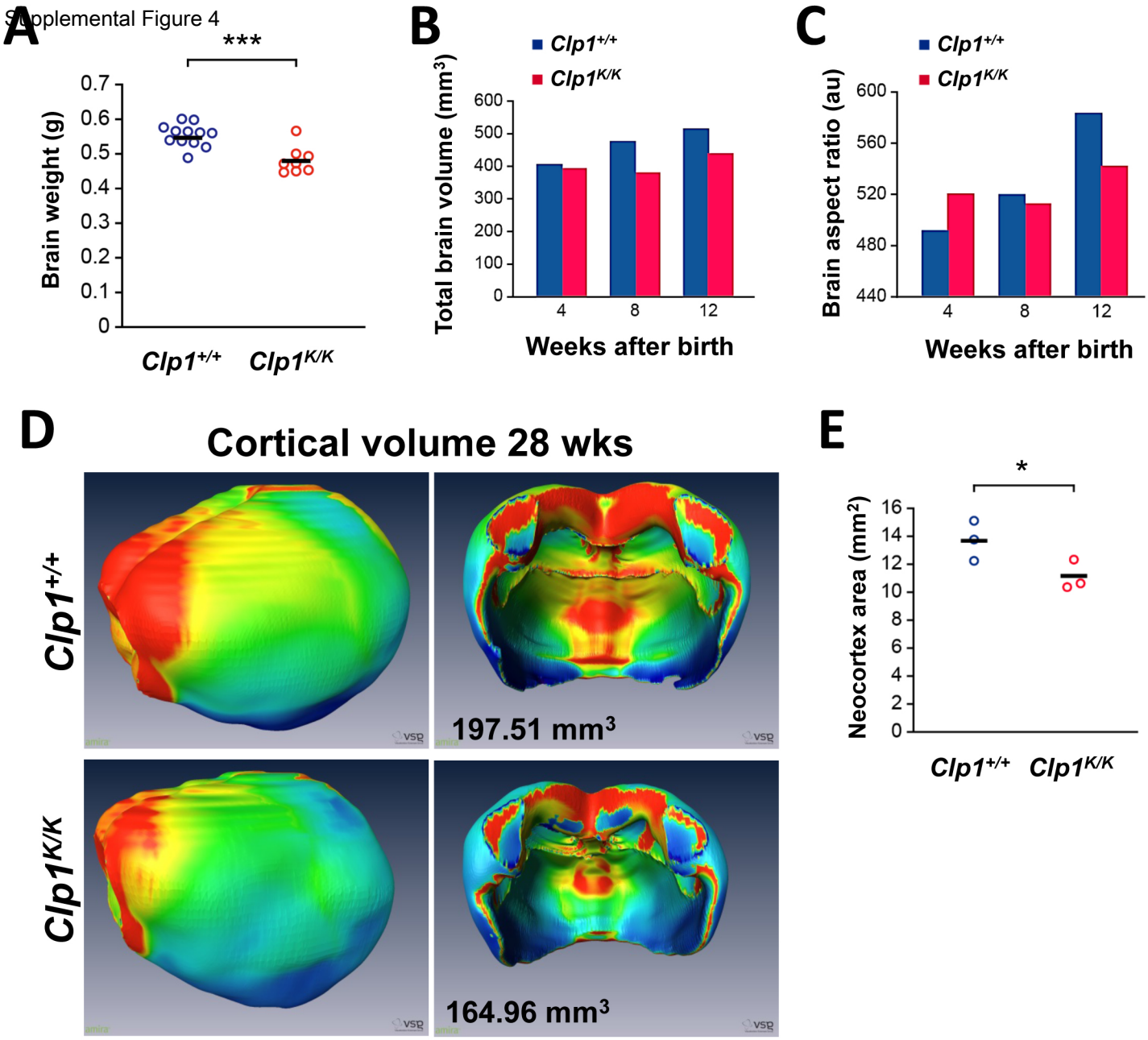

Supplementary Figure 4

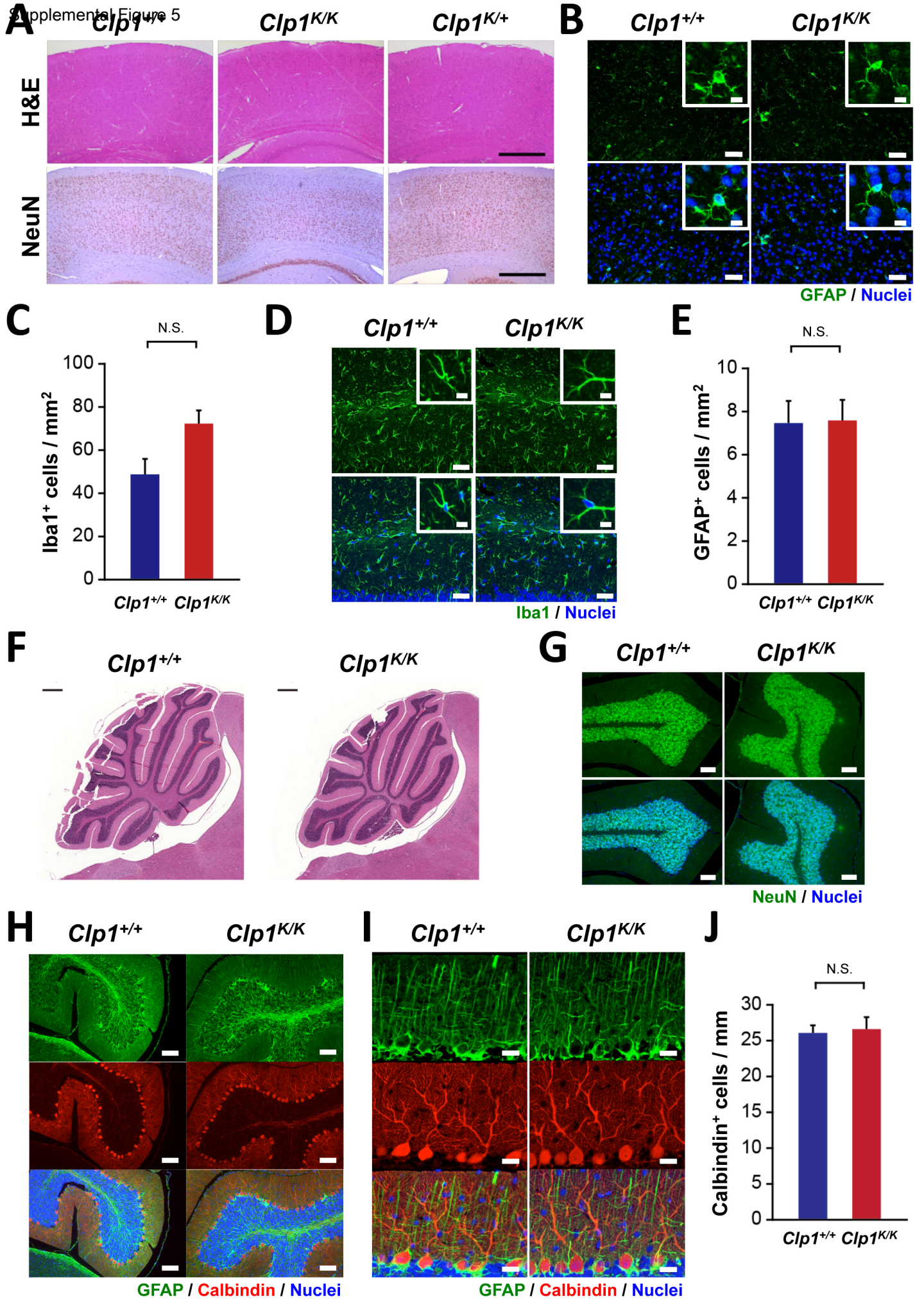

Supplementary Figure 5

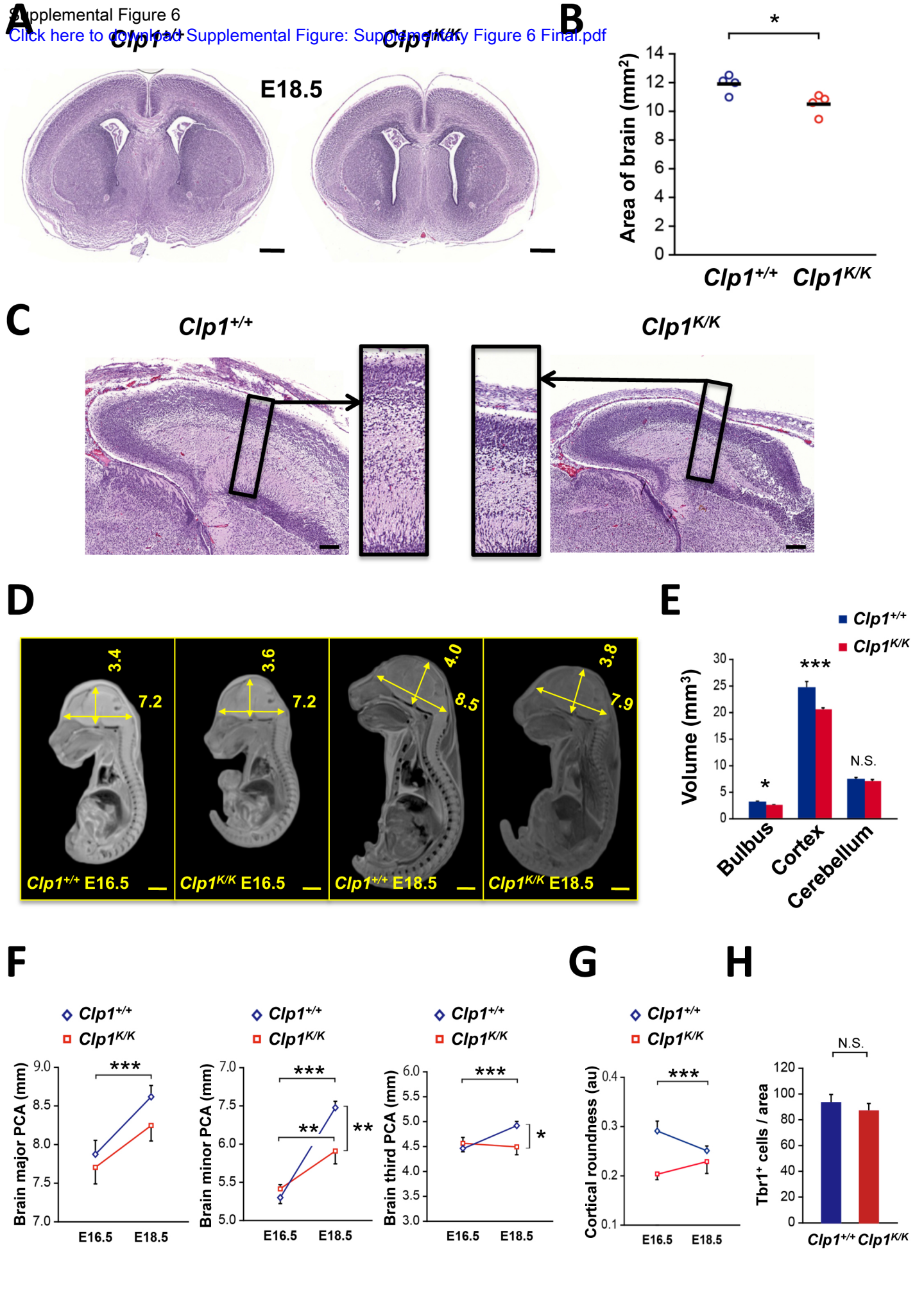

Supplementary Figure 6

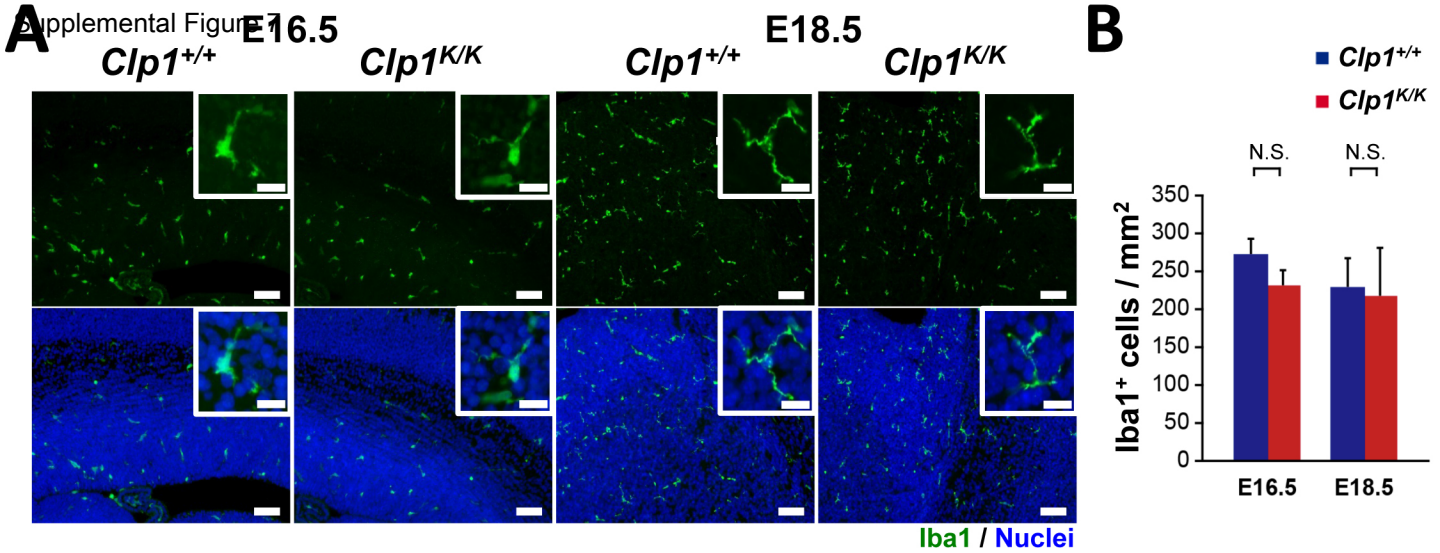

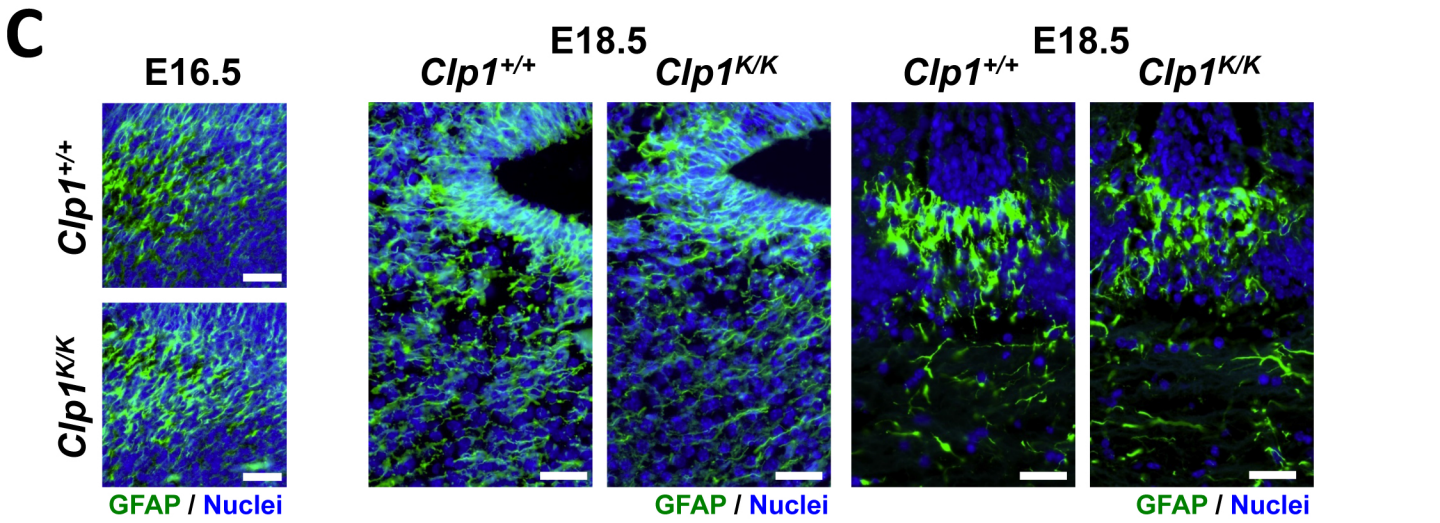

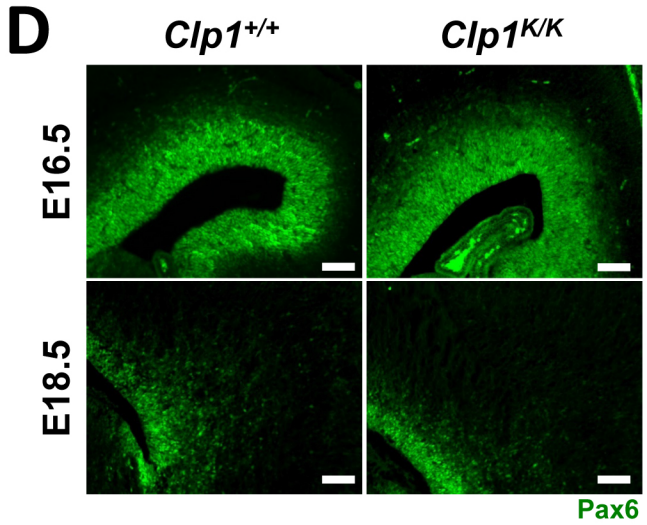

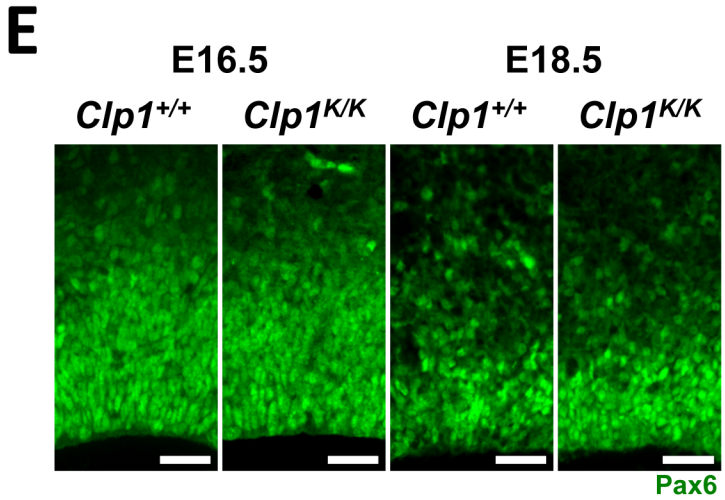

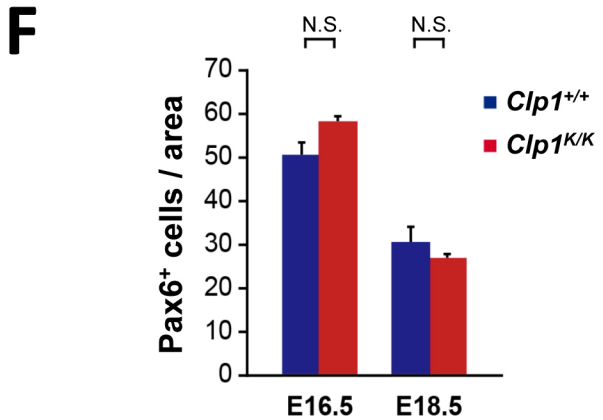

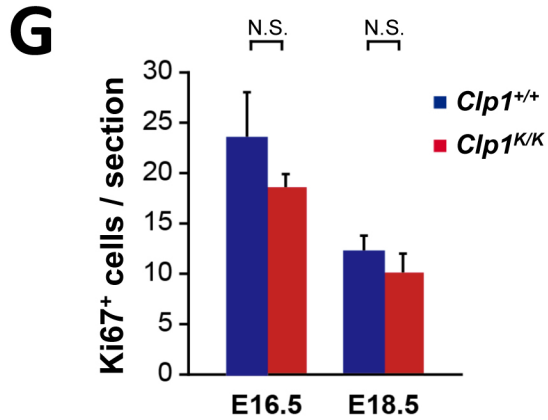

Supplementary Figure 7